Separation of Liquids by Thermal Diffusion

JOHN E. POWERS and C. R. WILKE

University of California, Berkeley, California

Data were obtained in flat-plate continuous-flow thermogravitational columns to check the theory developed by Furry, Jones, and Onsager and a modification of this theory proposed by the authors. Separations of ethyl alcohol–water and benzene–*n*-heptane mixtures were measured, flow rate, column length, temperature difference, spacing between plates, and inclination of the plates being varied in the experiments. Theory and data are in qualitative agreement for the range of variables studied. Quantitative agreement exists between theory and experiment in the region of practical design for liquid-thermal-diffusion plants.

Equations to aid in the design of thermal-diffusion plants are developed, and a plant to treat 1,000 bbl./day of a liquid aromatic-aliphatic mixture is designed and costs are estimated.

During the past quarter century the need for new separation methods, particularly for commercial application, has given strong impetus to the investigation of irreversible processes. For example, most of the work on irreversible processes involving nonisothermal-solution behavior has been reported in the past several decades, although this effect was first noted almost one hundred years ago.

Nonisothermal solution behavior has two manifestations, one the inverse of the other. If two gases of different composition and initially at the same temperature are allowed to diffuse together, a transient temperature gradient results from the ordinary diffusion process. This phenomenon was first noted by Dufour (*4*) in 1873, and bears his name. Conversely, if a temperature gradient is applied to a homogeneous solution, a concentration gradient is usually established. The name *thermal diffusion* (or *thermodiffusion*) is generally applied to this second effect.

Obviously only the nonisothermal-solution phenomena relating to thermal diffusion can be used for the separation of solutions, as the Dufour effect is the result of a mixing process. Two methods of utilizing thermal diffusion for the separation of solutions have been proposed. In the static method the thermal gradient is established in such a manner that convection is eliminated and there is no bulk flow. When applied to liquid or solid solutions the static method is called the Ludwig-Soret, or the Soret, effect. No special name has been given to the phenomenon in gases. The extent of the separation obtainable by the static method is generally very slight. The thermogravitational method multiplies the separation achieved in the static method by utilizing convection currents to produce a cascading effect. The apparatus that is used to produce the cascading effect is called a *thermogravitational* column or, commonly, a Clusius-Dickel column (*3*). Thermogravitational columns have been used to bring about separations in both gas and liquid solutions and have been operated in both batch (not to be confused with static) and continuous manners. The terms *continuous* and *batch* indicate, respectively, the presence or absence of a net bulk flow through the thermogravitational column.

Numerous reviews on thermal diffusion are available (*1, 5, 10*). The diversity of nationality represented by these publications attests to the widespread attention given to the subject. Several of these reviews merit particular discussion.

DeGroot (*5*) has presented a very comprehensive study of thermal diffusion in condensed phases (liquids and solids). His review of the theories that have been applied to the fundamental problem of the Soret effect is excellent, although he recognizes that these theories have met with very limited success, an article by Jones and Furry (*10*), which contains a resume of the theories and experimental work published before 1946, is especially noteworthy because of its excellent summary of column theory. Theoretical treatments of hot-wire, concentric-cylinder, and flat-plate columns are included, and the transient and steady state behavior of batch columns with and without reservoirs are discussed. The results obtained from the theoretical treatment of a batch column are extended to continuous-flow apparatus, and both single- and multistage processes are considered. The authors point out that the equations developed by Furry, Jones, and Onsager (*7*) for gas separations are equally applicable to the treatment of liquids.

Continuous-flow thermogravitational columns would most certainly be used in any large-scale commercial application of thermal diffusion. The equations for such columns reviewed by Jones and Furry incorporate a large number of assumptions and yet no critical comparison of theory and experimental data has appeared in the literature. It is the purpose of this study to compare theory with experimental data on continuous-flow columns and to improve on the theory where possible.

COLUMN THEORY

The temperature gradient applied between the plates of a thermogravitational column has two effects: (1) a flux of one component of the solution relative to the other (or others) is brought about by thermal diffusion, and (2) convective currents are produced parallel to the plates owing to density differences. The combined result of these two effects is to produce a concentration difference between the two ends of the column which is generally much greater than that obtainable by the static method. Figure 1 illustrates the flows and fluxes prevailing in a continuous-flow column.

In an ideal column a temperature gradient exists only in the direction normal to the plates. The flux of component 1 due to thermal diffusion, J_{x-TD}, is given by (*10*)

$$J_{x-TD} = \frac{\alpha D}{T} C_1 C_2 \frac{dT}{dx} \qquad (1)$$

The choice of sign is arbitrary and is taken as positive in order to be consistent with the notation of Jones and Furry (*10*). Equation (1) was developed to represent the behavior of isotopic gas mixtures. In this case α is essentially independent of temperature, pressure, and composition. Although nonisotopic liquid solutions may bear little resemblance to isotopic mixtures of gases,

J. E. Powers is at present at The University of Oklahoma, Norman, Oklahoma.

Equation (1) can be used to define the thermal-diffusion constant α for liquids.

The concentration gradient produced by the combined effects of thermal diffusion and convection acts to oppose thermal diffusion and limits the separation. By combining the thermal-diffusion flux with simultaneously acting fluxes due to ordinary diffusion and convective flow the general differential equation applicable to any point in the column may be formulated:

$$\frac{\partial C_1}{\partial t} = D\left[\frac{\partial^2 C_1}{\partial x^2} + \frac{\partial^2 C_1}{\partial y^2}\right] - \frac{\alpha D}{\bar{T}}\frac{dT}{dx}\frac{\partial (C_1 C_2)}{\partial x} - v(x)\frac{\partial C_1}{\partial y} \qquad (2)$$

Only the steady state solution of this equation ($\partial C_1/\partial t = 0$) is considered in this article.

The net flow due to thermal diffusion and ordinary diffusion must be zero at both walls. Therefore a solution to Equation (2) must be found subject to the boundary conditions

$$-D\frac{\partial C_1}{\partial x} + \frac{\alpha D}{\bar{T}} C_1 C_2 \frac{dT}{dx} = 0 \qquad (3)$$

at $x = \pm\omega$

In addition to the conditions expressed in Equation (3), a solution to Equation (2) must satisfy material balances made around any section of the column. Equation (4) represents a material balance made around the end of the enriching section.

$$\sigma_e C_e = +B_e \int_{-\omega}^{+\omega} \rho C_1 v(x)\, dx - B_e \int_{-\omega}^{+\omega} \rho D \frac{\partial C_1}{\partial y}\, dx \qquad (4)$$

Equation (5) expresses a similar condition existing in the stripping section:

$$-\sigma_s C_s = +B_s \int_{-\omega}^{+\omega} \rho C_1 v(x)\, dx - B_s \int_{-\omega}^{+\omega} \rho D \frac{\partial C_1}{\partial y}\, dx \qquad (5)$$

The velocity distribution $v(x)$ appearing in Equations (2), (4), and (5) is determined by applying the Navier-Stokes relations for laminar flow. For the enriching section:

$$v(x) = \frac{\beta_T g \cos\theta \Delta T}{12\omega\eta}(\omega^2 x - x^3) + \frac{3}{4}\frac{\sigma_e}{B_e \rho \omega^3}(\omega^2 - x^2) \qquad (6)$$

In obtaining a solution to these equations for a batch column ($\sigma_e = \sigma_s = 0$) Furry, Jones, and Onsager (*7*) assumed $\partial C/\partial y$ in Equations (2), (4), and (5) to be independent of x. (For a complete listing of the assumptions see reference *14*.) Based on this assumption the following relation was obtained:

$$q = \exp\left[\frac{H^{(0)} L_T}{K^{(0)}}\right] \qquad (7)$$

$$H^{(0)} = \frac{\alpha\beta_T \rho g \cos\theta (2\omega)^3 B_e (\Delta T)^2}{6!\eta\bar{T}} \qquad (7a)$$

$$K^{(0)} = K_c^{(0)} + K_d \qquad (7b)$$

$$K_c^{(0)} = \frac{\beta_T{}^2 \rho g^2 \cos^2\theta (2\omega)^7 B (\Delta T)^2}{9! D\eta^2} \qquad (7c)$$

$$K_d = 2\omega D B_e \rho \qquad (7d)$$

The assumption that $\partial C/\partial y$ is independent of x is incompatable with the boundary conditions, Equation (3), in the case of a continuous-flow column. To obtain a solution for this case it was necessary (*7*) to set $\sigma_e = 0$ in Equation (6) but not in Equation (4). For these conditions Jones and Furry (*10*) list a general solution and a number of restricted solutions. For the conditions of this experimental investigation, namely,

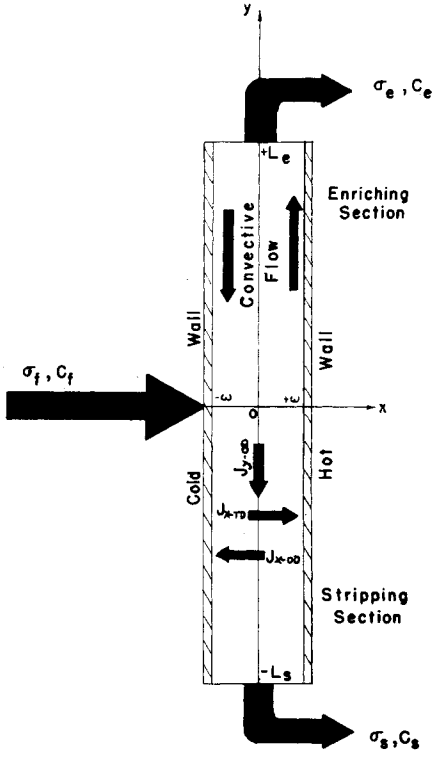

Fig. 1. Schematic diagram of a continuous-flow thermogravitational column.

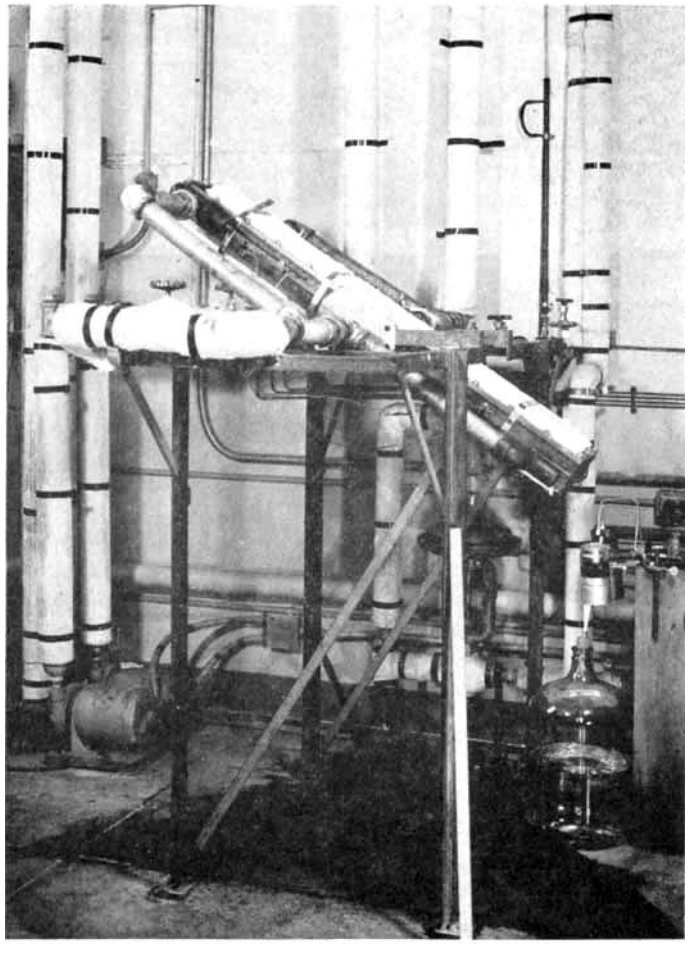

Fig. 2. Thermogravitational column (4 ft.) at an angle of 45 deg.

$C_1C_2 = \cong 0.25$; i.e., $0.7 > C_1 > 0.3$

$\sigma_e = \sigma_s \equiv \sigma$

$L_e = L_s = L_T/2$

$B_e = B_s$

the solution for a continuous-flow column is*

$$\Delta \equiv C_e - C_s = \frac{H^{(0)}}{2\sigma}\left(1 - \exp\frac{-\sigma L_T}{2K^{(0)}}\right) \quad (8)$$

In an attempt to improve on the equations for the continuous-flow thermogravitational column, it was assumed in the course of this work that $\partial C/\partial y$ was not independent of x but varied linearly; i.e.,

$$\partial C/\partial y = (1 + \gamma x)\psi(y) \quad (9)$$

This assumption made it possible to include the bulk-flow-rate term in Equations (4) and (6) and to satisfy the boundary conditions imposed by Equation (3). Completing the derivation yields an equation similar to (8):

$$\Delta = \frac{H}{2\sigma}\left(1 - \exp\frac{-\sigma L_T}{2K}\right) \quad (10)$$

where

$$H = H^{(0)}h(\omega\gamma) \quad (11)$$

$$h(\omega\gamma) = 1 - 18 \cdot \sum_{\lambda=0}^{\infty} \frac{(\omega\gamma)^{2\lambda}}{(2\lambda-1)(2\lambda+1)(2\lambda+3)(2\lambda+5)} \quad (12)$$

$$K = K_c{}^{(0)}k(\omega\gamma) + K_d \quad (13)$$

*More generally over any interval for which C_1C_2 can be assumed constant at $\overline{C_1C_2}$,

$$\Delta = \frac{2\overline{C_1C_2}H^{(0)}}{\sigma}\left(1 - \exp\frac{-\sigma L_T}{2K^{(0)}}\right)$$

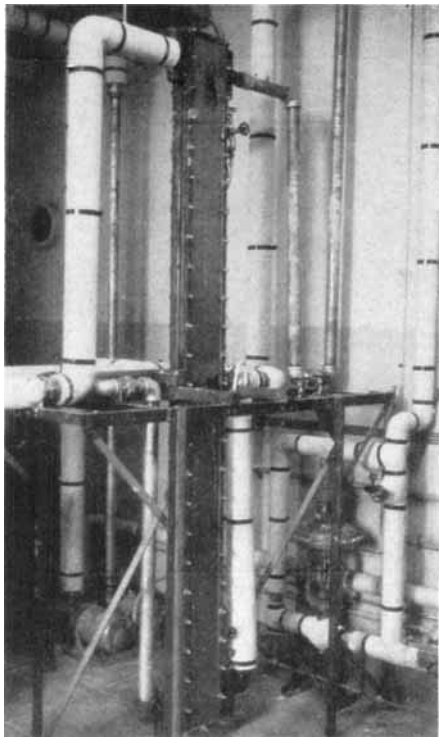

Fig. 3. Thermogravitational column (8 ft.) in the vertical position.

TABLE 1. SEPARATION AND FLOW-RATE MEASUREMENTS FOR THE SYSTEM ETHYL ALCOHOL–WATER

Experiment and group	σ_e Flow rate, g./min. Top product	σ_s Flow rate, g./min. Bottom product	σ $(\sigma_e + \sigma_s)/2$, g./min.	C_e Composition, weight fraction EtOH Top product	C_s Composition, weight fraction EtOH Bottom product	Δ $C_e - C_s$, weight fraction EtOH	ΔT Temp. diff., °C.
94-Q	10.55	9.5	10.025	0.3982	0.3913	0.0069	35.4
102-R	9.95	9.9	9.9	0.4026	0.3910	0.0116	36.4
111-S	1.71	1.47	1.59	0.4090	0.3851	0.0239	35.7
134-W	13.55	14.3	13.9	0.3986	0.3982	0.0004	36.2
139-X	0.853	0.814	0.834	0.4087	0.3893	0.0194	18.0

TABLE 2. SEPARATION AND FLOW-RATE MEASUREMENTS FOR THE SYSTEM *n*-HEPTANE–BENZENE

Experiment and group	σ_e Flow rate, g./min. Top product	σ_s Flow rate, g./min. Bottom product	σ $(\sigma_e + \sigma_s)/2$, g./min.	C_e Composition, mole fraction nC_7 Top product	C_s Composition, mole fraction nC_7 Bottom product	Δ $C_e - C_s$, Mole fraction nC_7	ΔT Temp. diff., °C.
177-BA	2.03	1.90	1.96	0.528	0.461	0.067	38.9
178-BA	1.37	1.04	1.20	0.529	0.456	0.073	38.9
186-BB	1.45	1.90	1.67	0.531	0.482	0.049	42.2
187-BB	8.7	9.2	8.95	0.522	0.487	0.035	42.2
193-BC	9.5	9.9	9.7	0.511	0.490	0.021	43.7
194-BC	1.9	1.8	1.85	0.549	0.452	0.097	43.2

$$k(\omega\gamma) = 1 - 0.39636(\omega\gamma)^2 + 0.09844(\omega\gamma)^4 \sum_{\lambda=0}^{\infty}(\omega\gamma)^{2\lambda} \sum_{n=0}^{6}\frac{\binom{6}{n}(-1)^n}{2n + 2\lambda + 1} \quad (14)$$

$$\gamma = \frac{-6!\eta\sigma_e}{(2\omega)^4\beta_T\rho g \cos\theta B_e \Delta T} \quad (15)$$

The infinite series in Equations (12) and (14) converge in the interval $|\omega\gamma| \leq |1|$.

Equations (8) and (10) referred to as the *uncorrected* and the *corrected* equations respectively, are compared with experimental data in a later section. These equations have the simplest form of any of the solutions presented by Jones and Furry and are as valid as the more general equation in the region for which they were developed.

EXPERIMENTS

Continuous-flow Thermogravitational Column

Equipment. The two thermogravitational columns used in the course of this investiga-

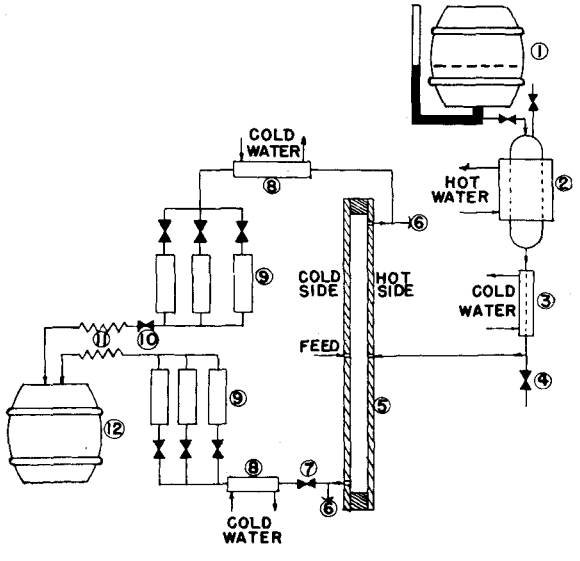

Fig. 4. Gravity-flow feed system: (1) feed barrel, (2) out-gasser, (3) feed cooler, (4) feed-sample tap, (5) thermogravitational column, (6) product-sample taps, (7) control valve, (8) product coolers, (9) rotameters, (10) control valve, (11) shunted capillary tubes, and (12) product barrel.

tion were constructed in the form of parallel plates (rather than concentric cylinders) in order to facilitate changes in the plate spacing (2ω) and to permit operation of the column at angles other than vertical. The working space between the plates measured approximately 6 in. by 4 ft. in the smaller column and 6 in. by 8 ft. in the larger. The transfer plates were constructed of 1/8-in. stainless steel sheet that was relatively free of scratches. The surfaces of these plates were given no special finishing treatment, as grinding caused excessive warpage of the plates. Two thermocouples were located on the surface of each transfer plate. The column was supported on an iron frame by means of support arms, to one of which a pointer was attached to indicate the angle of the column on a large metal protractor connected to the frame. Figure 2 is a view of the 4-ft. column inclined at an angle of 45 deg. and Figure 3 is a photograph of the 8-ft. column.

The gravity-flow feed system that provided steady flows through the columns is diagramed in Figure 4. All material other than the gasket contacted by the feed was either stainless steel, glass, or Teflon. The feed supply was kept in a barrel (1) 14 ft. above the floor. The liquid level in the barrel could be seen in a glass side tube. The feed was raised to the temperature of the heating water in a 1-liter glass cylinder (2) just below the feed barrel. The gases released by this heating process were periodically vented from the cylinder. The feed was cooled on passing through a small heat exchanger (3), and a sample tap (4) was located between the feed cooler and the thermogravitational column (5). The feed entered the column through holes drilled centrally in both transfer plates. The top product was removed through the hot plate and the bottom product through the cold plate. Product sample taps (6) were located as close to the working space as possible.

Temperature-controlled water was circulated through jacketed sections on either side of the transfer plates to control the temperature at the hot and cold walls.

Procedure. In experiments with the continuous-flow thermogravitational columns, the separation was determined as a function of flow rate. The plate spacing 2ω, column length L_T, angle of plates from the vertical θ, and temperature difference between the plates ΔT were treated as parameters. Changes in θ and ΔT could be made easily. Two separate columns were used to investigate the effect of column length. The plate spacing was varied by using gaskets of different thicknesses between the transfer plates. After a new gasket had been installed the plate spacing had to be determined accurately before the more useful experimental data could be taken. As the plate spacing appears in the theory as $(2\omega)^3$, $(2\omega)^4$, and $(2\omega)^7$, interpretation of the data is extremely sensitive to any error in this measurement. The method of measuring the plate spacing is discussed in detail elsewhere (*14*). Table 3 lists typical measured values of the column parameters, as well as average values of the feed composition and column width.

After necessary plate-spacing determinations had been made, a series of experiments was conducted to determine the separation as a function of the flow rate. The column and all lines were purged with the mixture to be investigated. The rotameters were used to set approximate flow rates through the working space, and samples from both product streams were analyzed periodically. Sufficient time was allowed between sets of samples to purge the headers and eliminate any disturbances introduced by the sampling procedure. The separation was

TABLE 3. MEASURED VALUES OF COLUMN PARAMETERS

Group	Included runs	Plate spacing from direct measure 2ω, cm.	Mean temp. diff. ΔT_m, °C.	Angle‡ from vertical θ, °	Total column height L_T, cm.	Column width B, cm.	Feed conc. C_F
Q	94–101	0.1356–0.1344*	35.2	+1.0	115.8	15.32	0.3933–0.3962
R	102–110	0.1454–0.1378*	37.0	+1.0	237.8	15.30	0.3977
S	111–115	0.1344†	35.9	+1.0	237.8	15.30	0.3982
W	134–138,145 149–152,164	0.0908†	36.0	+1.0	237.8	15.17	0.3986
X	139–142	0.0908†	18.1	+1.0	115.8	15.17	0.3986
BA	177–184	0.0813	41.1	+1.0	115.8	15.17	0.492
BB	186–192	0.1078†	42.1	+1.0	115.8	15.59	0.502
BC	193–200	0.0805†	43.0	+1.0	115.8	15.66	0.500

*Extremes of measured values.
†Average value (data self-consistent).
‡Positive angles indicate hot plate on top.

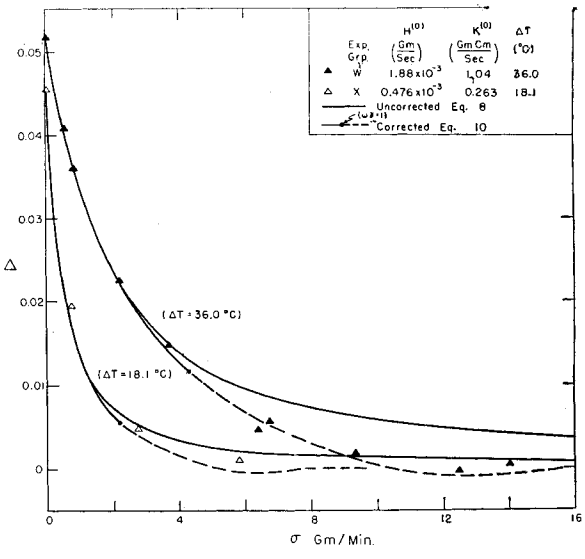

Fig. 5. Separation in a continuous-flow thermogravitational column as a function of flow rate.

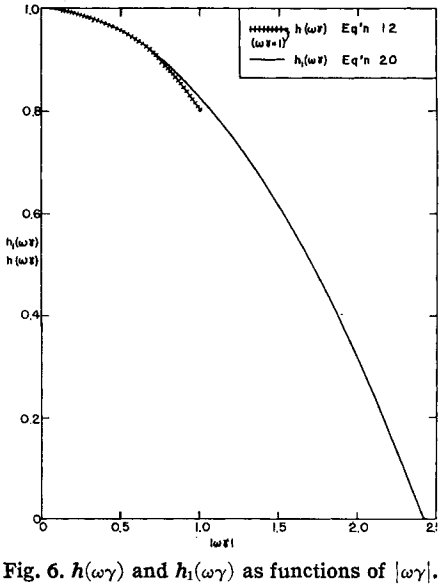

Fig. 6. $h(\omega\gamma)$ and $h_1(\omega\gamma)$ as functions of $|\omega\gamma|$.

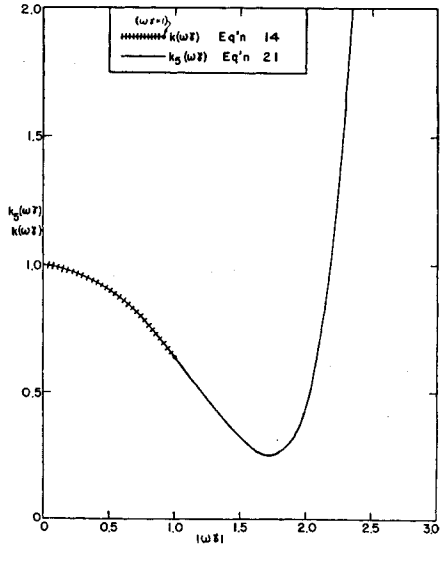

Fig. 7. $k(\omega\gamma)$ and $k_5(\omega\gamma)$ as functions of $|\omega\gamma|$.

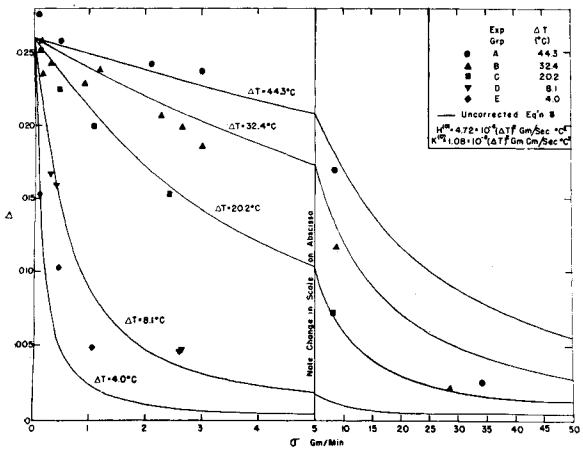

Fig. 8. Separation as a function of flow rate with temperature difference as parameter.

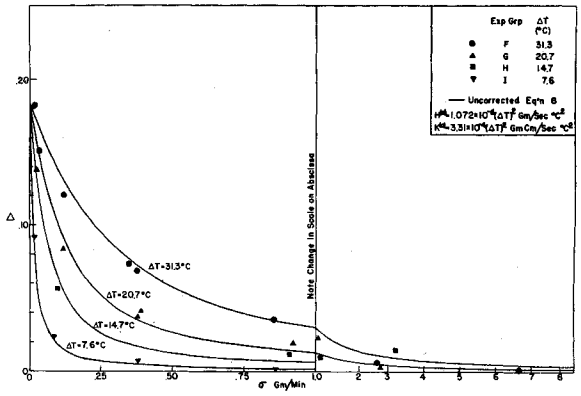

Fig. 9. Separation as a function of flow rate with temperature difference as a parameter.

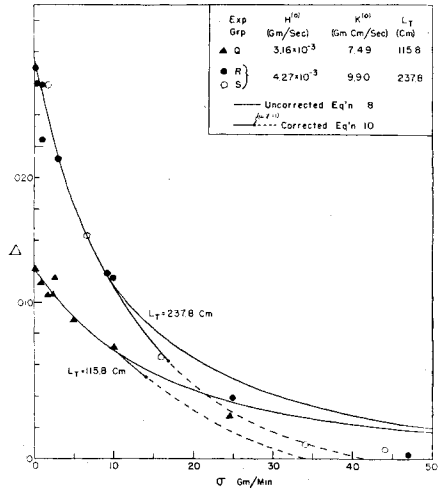

Fig. 10. Separation as a function of flow rate with column length as parameter.

plotted as a function of the time to determine the steady-state separation when the relaxation time was large compared with the time between samples. Several analyses were made with the column operating under steady state conditions, and the average of these analyses was reported. During the time interval between samples taken under steady state conditions, rotameter readings were taken, and the actual product-flow rates were measured by collecting and weighing samples. Other readings taken at this time included the temperatures of the water entering and leaving the column, manometer readings (water flow rate), controller readings, index of refraction of the feed, feed-barrel level, and the potentials of the four thermocouples located at the surfaces of the transfer plates. A record of these four potentials was made by a Brown electronic multipoint recorder.

All experiments with the ethyl alcohol-water system were made at a mean temperature level of 120°F., and those made with the *n*-heptane–benzene mixtures were at a mean temperature of 108°F. These mean temperatures were taken as the average of the temperatures indicated on the temperature recorder-controllers. Physical properties of the materials are given in Table 4. Concentrations were determined from refractive-index measurements of the solutions based upon calibration data obtained on reference solutions of the materials used in the columns.

RESULTS

Typical results are given in Table 1 for the ethyl alcohol–water system and

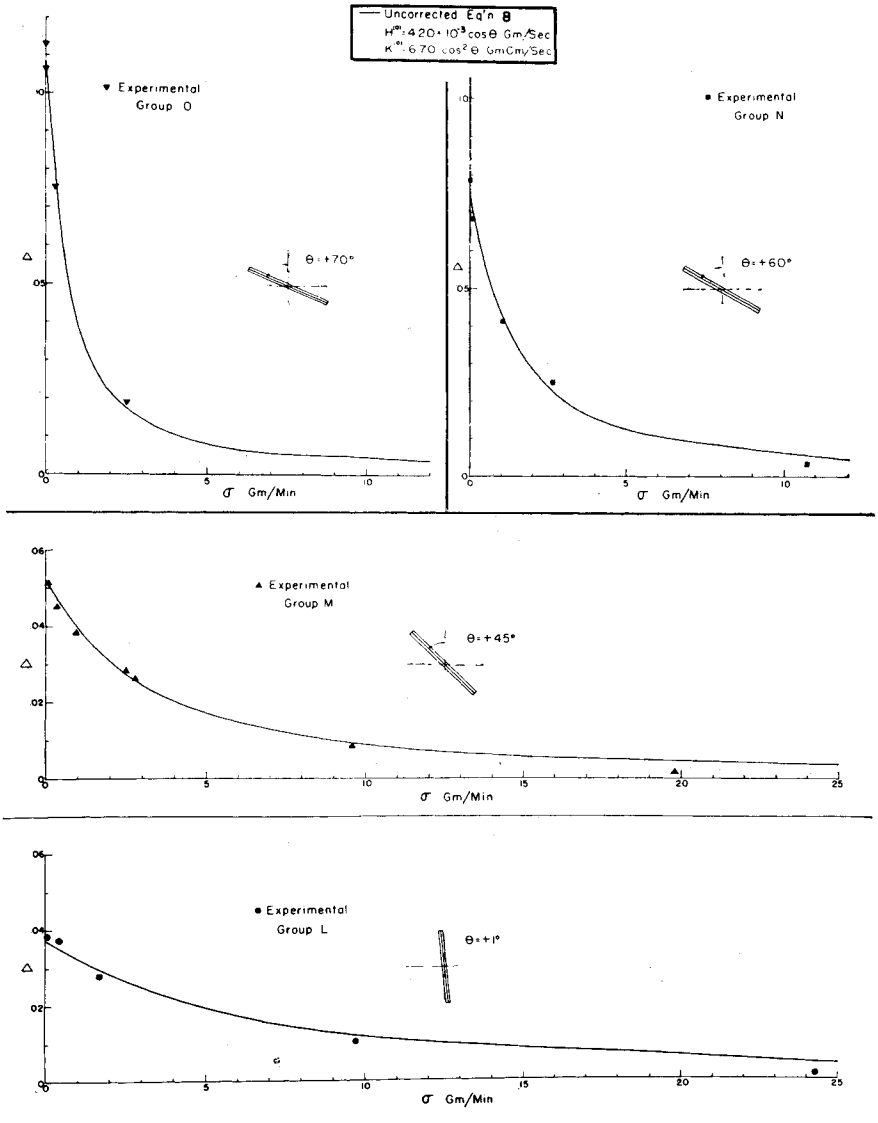

Fig. 11. Separation as a function of flow rate with column inclined at various angles.

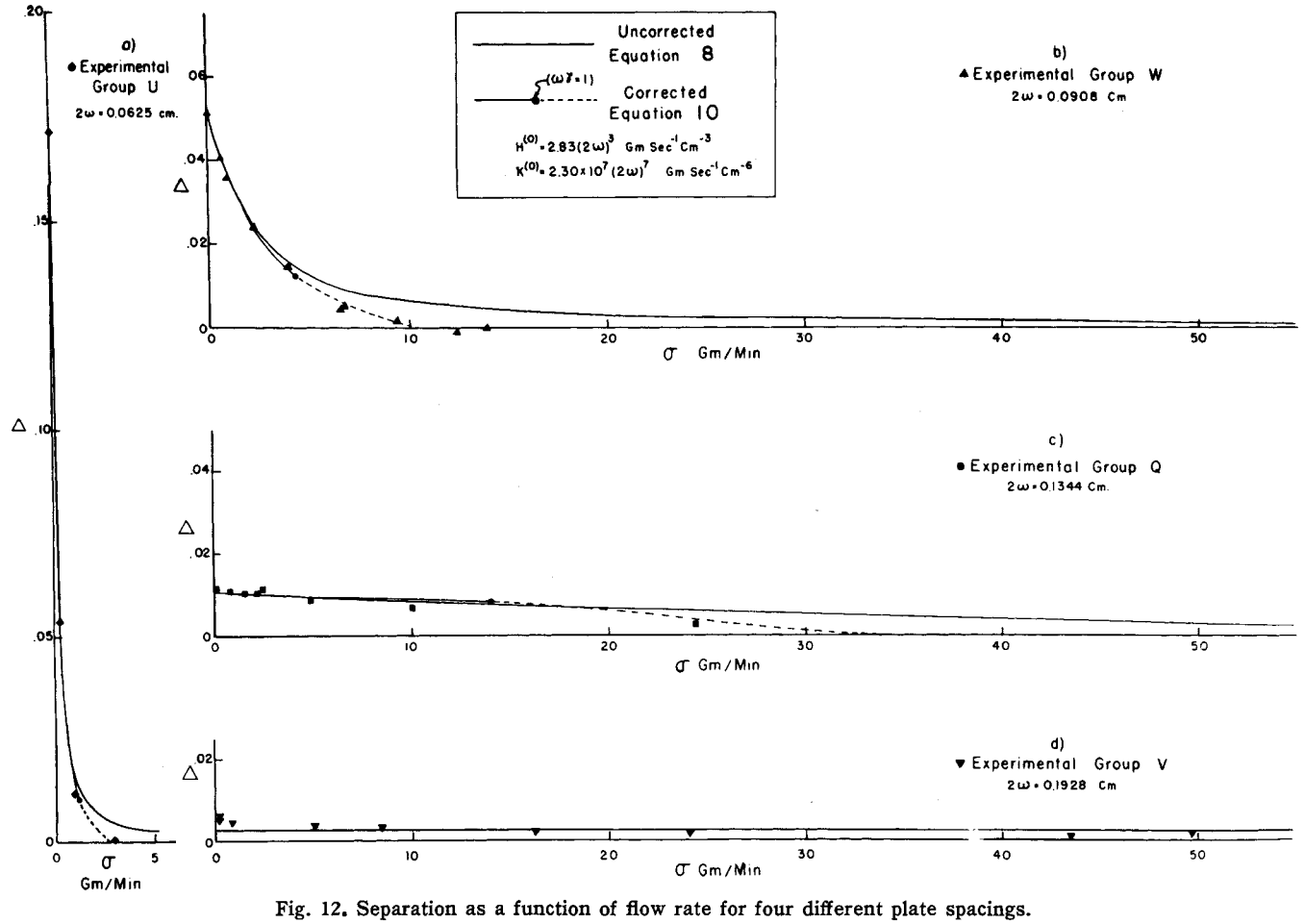

Fig. 12. Separation as a function of flow rate for four different plate spacings.

in Table 2 for the *n*-heptane–benzene system. (A complete listing of the data is on file.*) Included in the original thesis (*14*) are data on the column heat load and approach to steady state in the columns.

INTERPRETATION OF EXPERIMENTAL RESULTS

The mixtures investigated in the continuous-flow thermogravitational columns were all relatively concentrated binary liquid solutions. This type of mixture was chosen for several reasons: (*a*) there are relatively few data on such systems reported in the literature; (*b*) the maximum separation of any ideal binary mixture should occur when the feed is composed of equal amounts of each component; and (*c*) for the conditions $0.7 > C_1$ 0.3, i.e., for $C_1C_2 \cong \frac{1}{4}$, the solution to the transport equation is of the simple form given by Equations (8) and (10).

Flow-rate Dependence

Two of the first questions to be resolved were whether the flow-rate dependence predicted by Equations (8) and (10) corresponded to the experimental results and over what range the uncorrected equations of Jones and Furry (*10*) were applicable. Since the flow-rate dependence is here considered to be of prime importance, values of $H^{(0)}$ and $K^{(0)}$ in Equations (8) and (10) were determined empirically in such a manner that Δ values calculated from these equations agreed with experimental data in the region $\sigma \rightarrow 0$. The following procedure was used to obtain empirical values of $H^{(0)}$ and $K^{(0)}$. If Equation (10) is expanded in series, Equation (16) results:

$$\Delta = \frac{HL_T}{4K} - \frac{HL_T^2}{8K^2}\sigma + \frac{HL_T^3}{16K^3}\sigma^2 \cdots \quad (16)$$

In the limit $\sigma \rightarrow 0$, the intercept Δ_0 and the initial slope m_0 are obtained from Equation (16) by inspection.

$$\Delta_0 = \frac{H^{(0)}L_T}{4K^{(0)}} \quad (17)$$

$$m_0 = -\frac{H^{(0)}L_T^2}{8(K^{(0)})^2} \quad (18)$$

Equations (17) and (18) can thus be solved simultaneously for $H^{(0)}$ and $K^{(0)}$ values that will satisfy the experimental values of Δ_0 and m_0.

Some typical data are presented in Figure 5. The complete solid lines represent values of the separation Δ calculated from uncorrected Equation (8) with values of $H^{(0)}$ and $K^{(0)}$ determined in the manner described in the preceding paragraph. The solid lines ending in a dot represent separations calculated from the corrected Equation (10) by use of these same $H^{(0)}$ and $K^{(0)}$ values. For relatively low flow rates the corrected and uncorrected equations give almost identical results and agree very well with the data. At higher flow rates the uncorrected equation deviates markedly from the data and predicts separations larger than those found experimentally. The corrected equation gives values that compare very well with the experimental data. However, for values of $\omega\gamma > 1$ (dots indicate $\omega\gamma = 1$) the series appearing in Equations (12) and (14) diverge and lead to the indeterminant expression $\Delta = \infty \cdot 0$.

It is of interest to note that in all cases tested the unmodified theory, Equation (8), is in fair agreement with the data up to a flow rate corresponding to $\omega\gamma = 1$ and in poor agreement for higher flow rates. Thus the limit of applicability of Equation (8) is given by

$$(\sigma)_l = \frac{2(2\omega)^3\beta_T g \cos\theta B_e \Delta T}{6!\eta} \quad (19)$$

This further suggests that the $\omega\gamma$ term might be used to correlate correction factors similar to Equation (12) and (14) outside of the region of convergence of these series.

*Tabular material has been deposited as document 5209 with the American Documentation Institute, Photoduplication Service, Library of Congress, Washington 25, D. C., and may be obtained for $1.25 for photoprints or 35-mm. microfilm.

The dashed lines drawn as a continuation of the corrected curves on Figure 5 represent the use of correction terms $h_1(\omega\gamma)$ and $k_5(\omega\gamma)$. Values of $h_1(\omega\gamma)$ are calculated by ignoring all terms but the first in the series appearing in Equation (12), and $k_5(\omega\gamma)$ values are calculated by considering only the first five terms of the series in Equation (14). These relations are given by Equations (20) and (21) and are represented graphically in Figures 6 and 7.

$$h_1(\omega\gamma) = 1 - 0.17143(\omega\gamma)^2 \qquad (20)$$

$$k_5(\omega\gamma) = 1 - 0.39636(\omega\gamma)^2 + .033567(\omega\gamma)^4 + 2.2378 \times 10^{-3}(\omega\gamma)^6 + 3.949 \times 10^{-4}(\omega\gamma)^8 + 1.0392 \times 10^{-4}(\omega\gamma)^{10} + 3.464 \times 10^{-5}(\omega\gamma)^{12} \qquad (21)$$

Values of $h(\omega\gamma)$ and $k(\omega\gamma)$ for $|\omega\gamma| \leq 1$ are included in Figures 6 and 7 for comparison.

The term $h_1(\omega\gamma)$ becomes negative at large flow rates, and the separations predicted for $\omega\gamma > 2.43$ are opposite in sign to Δ_0. The net result of the use of $k_5(\omega\gamma)$ is to limit the separations calculated for $\omega\gamma > 2.43$ to very small values. Negative separation values are shown in Figure 5. In other figures the dotted line representing the corrected Equation (10) is terminated at $\omega\gamma = 2.43$ because separations of opposite sign at higher flow rates have no physical significance. In most cases both calculated and measured separation values are equal to zero within experimental accuracy for $\omega\gamma > 2.43$. The agreement with experimental data for $2.43 > \omega\gamma > 1.0$ that is obtained by using these approximations is remarkable, as the use of the first several terms in these divergent series is entirely empirical.

Equations (17) and (18) were used to determine empirical values of $H^{(0)}$ and $K^{(0)}$ for most of the groups of experimental data which were obtained. The variation of the separation Δ with flow rate was properly accounted for by use of Equation (10). In general the corrected equation with the terms $h_1(\omega\gamma)$ and $k_5(\omega\gamma)$ was superior to the uncorrected equation in representing the data.

The separation–flow-rate data successfully represented by Equation (10) were obtained for a variety of operating conditions. The theory predicts the effect of changes in the operating conditions, and the empirical $H^{(0)}$ and $K^{(0)}$ values can be used to check these predictions. The functional dependence of the term $H^{(0)}$ is given by Equation (7a). $K^{(0)}$ is composed of three additive terms: $K_c^{(0)}$, representing the remixing effects due to the convective flow; K_d, which accounts for vertical diffusion; and K_p, a term appended to the theory to account for parasitic remixing effects. Fortunately, for the range of variables investigated in connection with this research, both K_d and K_p appear to be negligible when compared with $K_c^{(0)}$. In this case the functional dependence of $K^{(0)}$ is essentially given by Equation (7c), i.e., that for $K_c^{(0)}$.

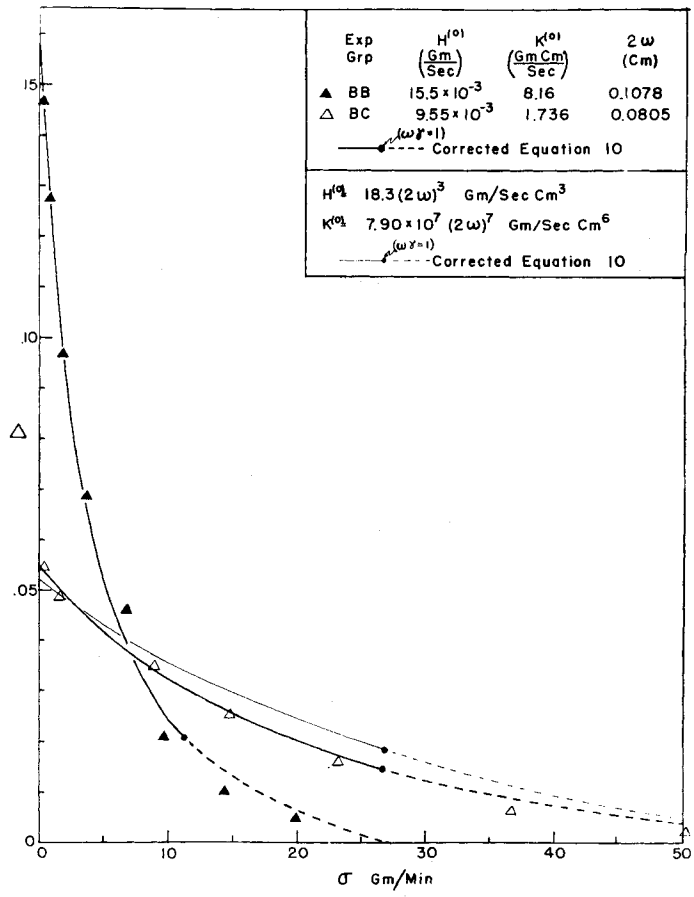

Fig. 13. Separation as a function of flow rate with plate spacing as parameter.

Temperature Difference (ΔT)

According to Equations (7a) and (7c), both $H^{(0)}$ and $K^{(0)}$ are proportional to $(\Delta T)^2$. Values of $H^{(0)}$ and $K^{(0)}$ used in Equation (10) were obtained from relations of the form $H^{(0)} = a(\Delta T)^2$ and $K^{(0)} = b(\Delta T)^2$ where a and b are empirical constants determined from the data. These relations seem to satisfy the data presented in Figures 5, 8, and 9 over a wide range of ΔT and for three different values of the plate spacing, 2ω.

In Figures 8 and 9 and subsequent figures in which no curve (or curves) representing the corrected equation appears, the measurement of the plate spacing was too inaccurate to permit a proper evaluation of the correction.

Length (L_T)

The theory predicts that $H^{(0)}$ and $K^{(0)}$ are independent of the column length. From Equation (17) Δ_0 should be proportional to L_T and, according to Equation (10), the separation should become independent of height at high flow rates. These theoretical predictions are definitely substantiated by the data presented in Figure 10. The difference between the values of $H^{(0)}$ and $K^{(0)}$ used to represent the two experimental groups and the deviation of the theoretical curves at high flow rates is due in part to slight differences in the plate spacing and ΔT.

Effective Gravitational Field ($g \cos\theta$)

The effective gravitational field was changed by tilting the column in the manner illustrated in Figure 2. This variation is accounted for in the theory by the product $g \cos\theta$. The results of experiments made with the hot plate on top (positive angles) are presented in Figure 11. The curves drawn on Figure 11 represent separations calculated using values of $H^{(0)}$ and $K^{(0)}$ obtained from relations of the form $H^{(0)} = a\cos\theta$ and $K^{(0)} = b\cos^2\theta$ as predicted by theory.

Plate Spacing (2ω)

According to the theory the separation should show a strong dependence on the plate spacing with $H^{(0)} = a(2\omega)^3$ and $K^{(0)} = b(2\omega)^7$. The magnitude of this effect is even more clearly emphasized by the fact that m_0, the initial slope, is inversely proportional to $(2\omega)^{11}$. The tremendous effect of the plate spacing is illustrated in Figure 12 by retaining the same relative scales on the four graphs. The curves on Figure 12 represent values

calculated from Equation (10) with values of $H^{(0)}$ and $K^{(0)}$ determined from the foregoing relations. Values of a and b were determined from the data taken for $2\omega = 0.0908$ cm. (Figure 12*b*), and slight corrections were made for variations in ΔT. The agreement appears to be quantitative largely because the scales are small.

Actually some discrepancies exist between the theoretical and experimental values for data taken at the larger plate spacings. Figure 13 represents other data taken to investigate the effect of plate spacing and will serve to illustrate the nature of these discrepancies. If the constants a and b in the relations $H^{(0)} = a(2\omega)^3$ and $K^{(0)} = b(2\omega)^7$ are evaluated from the data taken at the smaller plate spacing (larger Δ_0), values of $H^{(0)}$ and $K^{(0)}$ calculated from these relations fail to represent the data taken at the larger plate spacing (light line). The predicted value of Δ_0 is somewhat smaller than that found experimentally, and experimental values of the separation at high flow rates are substantially smaller than the calculated values. On the other hand, values of $H^{(0)}$ and $K^{(0)}$ obtained empirically from each invividual set of data serve to represent the data very well (heavy lines).

Jones (*9*) has reported some qualitative conclusions based on an extensive investigation of the separation of liquids in continuous-flow thermogravitational columns. Although he does not indicate the nature of the dependence of the separation on the flow rate, his conclusions with regard to other variables are in general agreement with the theory and with the results of this investigation.

PROCESS DESIGN

In order to obtain quantitative agreement between the theory and experimental data it was necessary to apply empirical correction factors to the terms $H^{(0)}$ and $K^{(0)}$. The correlation of these correction factors which was developed incorporates the data of Drickamer and his coworkers on the separation of mixtures of gases as well as mixtures of liquids. Details have been presented previously (*14*). From an engineering standpoint the most important conclusion to be reached from the correlation is that no correction or modification of the theory as originally proposed by Furry, Jones, and Onsager (*7*) and Jones and Furry (*10*) is necessary when their equations are used as the basis for design of thermal-diffusion plants for separation of liquid mixtures, because optimum design relations dictate the use of small plate spacings and low flow rates. The theory is in quantitative agreement with the data for these conditions.

Krasney-Ergen (*11*) has developed equations for estimating optimum dimensions in the design of thermal-diffusion processes based on the equations of Furry, Jones, and Onsager. Krasney-Ergen was interested principally in the concentration of relatively rare isotopes and treated the case in which the relative amount of the substance being concentrated, C_1, is very small throughout the apparatus ($C_1 \ll 1$). The equations "tested" in the present work, on the other hand, were based on the assumption that the materials being separated are present in almost equal amounts ($C_1C_2 \cong \frac{1}{4}$). In the next section the method of Krasney-Ergen will be applied to develop a design procedure for the case $C_1C_2 \cong \frac{1}{4}$.

Table 4. Values of Physical Properties Used in the Calculations

System A	System B	Fraction A	Average temp. $\bar{T}$, °K.	Density ρ, g./cc.	$-\partial\rho/\partial T \times 10^4$, g./(cc.)(°C.)	Diff. coef. $D \times 10^5$, sq. cm./sec.	Coefficient of viscosity η, centipoise
EtOH	H_2O	0.3986*	322.1	0.9133‡	8.11	1.04††	1.14**
EtOH	H_2O	0.3913*	322.1	0.9150‡	8.08	1.06††	1.12**
EtOH	H_2O	0.3322*	322.1	0.9273‡	7.80	1.262††	1.09**
n-Heptane	Benzene	0.500†	315.4	0.7363**	9.44	3.21‡‡	0.351¶

*Weight fraction.
†Mole fraction.
‡References *8* and *15*.
**Reference *8*.
††References *6*, *12*, and *16*.
‡‡Reference *18*.
¶Reference *17*.

EQUATIONS FOR DETERMINING THE OPTIMUM DIMENSIONS OF A THERMAL-DIFFUSION APPARATUS ($C_1C_2 \cong \frac{1}{4}$)

The optimum dimensions are the cheapest. Costs are considered in two categories only: (1) fixed charges, mainly depreciation of the capital investment, and (2) power costs, which are defined so as to include the cost of both fuel and cooling water. The notation S is used to denote the amount of fixed charges per unit area (square centimeters) per unit time (day). The amount of heat transferred is inversely proportional to the plate spacing, and therefore the power cost per square centimeter per day is designated by $p_c/2\omega$. The total cost π is given by

$$\pi = [S + p_c/2\omega] \int_A dA = [S + p_c/2\omega]BL_T \qquad (22)$$

From Equation (10),

$$L_T = \frac{2K}{\sigma}\left[-\ln\left(1 - \frac{2\sigma\Delta}{H}\right)\right] \qquad (23)$$

If the angle of the plates from the vertical θ is set arbitrarily and the temperature difference ΔT and temperature level $\bar{T}$ are dictated by the available heating and cooling media, for any particular system the terms $H^{(0)}$ and $K^{(0)}$ can be considered to be functions of the column width B and the plate spacing 2ω. [The terms $h(\omega\gamma)$ and $k(\omega\gamma)$ are ignored in this development.]

$$H^{(0)} = aB(2\omega)^3 \qquad (24)$$

$$K^{(0)} = a'B(2\omega)^7 + b'B(2\omega) \qquad (25)$$

Equation (26) is obtained by combining Equations (22) through (25):

$$\pi = \frac{2B^2}{\sigma}\left[a'S(2\omega)^7 + a'p_c(2\omega)^6 + b'S(2\omega) + b'p_c\right]\left\{-\ln\left[1 - \frac{2\sigma\Delta}{aB(2\omega)^3}\right]\right\} \qquad (26)$$

In general, the required separation Δ and the average flow rate σ are designated. The total cost π is then a function of 2ω and B only. From Equation (26) it can be shown that the costs are infinite in both of the limits $B \to \infty$ and $(2\sigma\Delta)/aB(2\omega)^3 \to 1.0$. Clearly then at least one minimum must exist between the limits defined by

$$0 > \frac{2\sigma\Delta}{aB(2\omega)^3} > 1.00 \qquad (27)$$

In order for the total cost to be minimized these conditions must be satisfied:

$$\frac{\partial\pi}{\partial B} = 0 = \frac{\partial\pi}{\partial(2\omega)} \qquad (28)$$

By differentiating Equation (26) with respect to B and combining with Equation (28), one obtains

$$-2\ln\left(1 - \frac{2\sigma\Delta}{aB^*(2\omega)^3}\right) = \frac{1}{\frac{aB^*(2\omega)^3}{2\sigma\Delta} - 1} \qquad (29)$$

B^* refers to the optimum value of the column width for any plate spacing.

The optimum plate spacing as a function of the various parameters is obtained by differentiating Equation (26) with respect to 2ω and combining the resulting equation with Equations (28) and (29):

$$(2^*\omega)^7 - 5\frac{b'}{a'}(2^*\omega) - 6\frac{b'}{a'}\frac{p_c}{S} = 0 \qquad (30)$$

Equation (30) is identical to the relation developed by Krasney-Ergen for the case $C_1 \ll 1$.

If Γ is defined by

$$\Gamma = \frac{2\sigma\Delta}{a(2\omega)^3} \tag{31}$$

Equation (29) can be reduced to

$$-2 \ln (1 - \Gamma/B^*) = \frac{1}{B^*/\Gamma - 1} \tag{32}$$

The solution to Equation (32) is

$$B^* = 1.39\Gamma \tag{33}$$

which is considerably more simple than the analogous relation developed by Krasney-Ergen.

DESIGN ILLUSTRATION

Both Krasney-Ergen (*11*) and Jones and Furry (*10*) have included numerical examples of the design of processes for concentrating dilute mixtures of isotopic gases. It is interesting to apply the equations developed in the preceding section to the design of a single-state apparatus for the separation of a concentrated liquid mixture.

For purposes of illustration a thermal-diffusion plant to process 1,000 bbl./day of a 50 mole % *n*-heptane–benzene mixture will be designed. This particular design would have no commercial significance, as *n*-heptane–benzene is easily separated by distillation. However, the process is indicative of separations of aromatics and aliphatics, a difficult separation when applied to lubricating oils.

Equation (10) used in this development was restricted to the range $0.7 > C_1 > 0.3$ and to equal flow rates in each section. On the basis of these restrictions the following product specifications were arbitrarily designated:

top product—
500 bbl./day 70 mole % *n*-heptane

bottom product—
500 bbl./day 30 mole % *n*-heptane

From these specifications it follows that $\Delta = 0.40$. The problem is further defined by setting $\cos\theta = 1.00$, $\Delta T = 100$°C. and $\bar{T} = 315$°K.

The power costs p_c were approximated by considering the cost of heating and cooling media to be twice the cost of fuel at 30 cents/million B.t.u. A value of \$7.32 × 10^{-6}/(day)(sq. cm./cm.) was obtained for p_c.

The equipment costs were assumed to be independent of 2ω and the cost per square foot of area of one plate was estimated to be \$60/sq. ft. This is ten times the value obtained from Chilton's (*2*) cost curves for heat exchange surface and is intended to include cost of auxiliary equipment, design, etc. On this basis a value of \$3.91 × 10^{-5}/(day)(sq. cm.) was obtained for S.

These cost data and values of the other system parameters were used in Equations (30), (31), (33), and (23) to obtain the dimensions for the "optimum" design listed in Table 5. Estimates of the total heat load, capital investment, and operating costs are included.

Even though a column 1.43 cm. long and 82.7 miles wide with a plate spacing of 0.182 mm. may be optimum, it would hardly seem practical. An increase in the plate spacing would decrease the column width and increase the column length. The cost would also be increased by any increase in plate spacing. (Actually a decrease in fabrication cost with an increase in 2ω would probably offset the predicted increase in cost.) A plate spacing of 0.793 mm. (1/32 in.) was arbitrarily chosen as a minimum practical plate spacing, and values of B and L_T were calculated from Equations (33) and (23). The results of these calculations are listed under Practical Design in Table 5 for comparison with the optimum design. The values of the column length (17 ft.) for this arbitrary plate spacing represent a practical construction, and thus no other designs were considered.

The cost data used in these estimates are certainly only approximate, and yet the results should indicate the order of magnitude of the costs. As pointed out previously, thermal diffusion is an expensive process; however, with motor oil selling for 60 cents a quart the process may become economically feasible in the near future.

Table 5. Summary of Design Estimates

Plant to process 1,000 bbl./day of 50 mole % *n*-heptane–benzene

	Optimum design	Practical design
2ω cm.	0.0182	0.0793
(in.)	(0.0072)	(1/32)
B, cm.	$1.33 \times 10^{+7}$	$1.60 \times 10^{+5}$
(ft.)	$(4.36 \times 10^{+5})$	$(5.25 \times 10^{+3})$
(miles)	(82.7)	(1.0)
L, cm.	1.43	514
(ft.)	(0.0468)	(16.9)
Total area		
($B \times L$), sq. cm.	$1.90 \times 10^{+7}$	$8.23 \times 10^{+7}$
(sq. ft.)	$(2.05 \times 10^{+4})$	$(8.88 \times 10^{+4})$
Heat load, B.t.u./hr.	$5.27 \times 10^{+8}$	$5.27 \times 10^{+8}$
Capital investment	\$1,230,000	\$5,320,000
Operating costs		
Fuel and cooling water	\$7,670	\$ 7,670
Fixed charges	743	3,230
Total	\$8,413	\$10,900
Cost per barrel of feed processed	\$8.41	\$10.90
Cost per gallon of feed processed	\$0.20	\$ 0.26

SUMMARY OF DESIGN PROCEDURES

Equations

Although there is some doubt as to the usefulness of the equations developed above in their application to liquids, they are summarized here for convenient reference.

Optimum Plate Spacing ($2^*\omega$)

$$(2^*\omega)^7 - 5\frac{b'}{a'}(2^*\omega) - 6\frac{b'}{a'}\frac{p_c}{S} = 0 \tag{30}$$

$$\frac{b'}{a'} = 9!\left(\frac{D\eta}{\beta_T g \cos\theta \Delta T}\right)^2 \tag{34}$$

Optimum Column Width (B^*)

$$B^* = 1.39\Gamma = \frac{2.78\sigma\Delta}{a(2\omega)^3} \tag{33a}$$

$$a = \frac{\alpha\beta_T\rho g \cos\theta(\Delta T)^2}{6!\eta\bar{T}} \tag{35}$$

Column Length (L_T^*)

$$L_T^* = \frac{2K^{(0)}}{\sigma}\left[-\ln\left(1 - \frac{2\sigma\Delta}{H^{(0)}}\right)\right] = \frac{2.54K^{(0)}}{\sigma} \tag{23a}$$

$$K^{(0)} = 2\omega DB^*\rho\left[\frac{a'}{b'}(2\omega)^6 + 1\right] \tag{36}$$

Determination of Design Constants

The equations listed above are most useful when applied to the separation of binary mixtures for which all the required data on the physical properties including the ordinary and thermal-diffusion coefficient are known. Under these conditions the application of the equations is straightforward, as was shown in the design illustration.

In general, not many of the required physical data are available even for binary systems. This is especially true of thermal-diffusion data. In this more general case the terms a, a', b', and $K^{(0)}$ can be evaluated empirically from data taken with either the continuous-flow or the batch-type thermogravitational column.

In the treatment of continuous-flow thermogravitational-column data, values of $H^{(0)}$ and $K^{(0)}$ would be obtained by use of Equations (17) and (18) as described. Values of $H^{(0)}$ and $K^{(0)}$ for batch columns are obtained from data on the approach to steady state in the column by applying the transient-state equations (*10*). (See also reference *13*.) In either case these $H^{(0)}$ and $K^{(0)}$ values can be used to determine a, a', and b' by applying Equations (24) and (25). Constants a' and b' can be determined from Equation

(25) by making several determinations at two different plate spacings.

In the light of present results it would appear that determination of $H^{(0)}$ and $K^{(0)}$ values to be used in any final design should be made in an apparatus with approximately the same plate spacing 2ω as that to be used in the plant. Further, when these constants are determined empirically, this design procedure can be applied also to the treatment of multicomponent mixtures.

ACKNOWLEDGMENT

The authors have become indebted to many people during the course of the work on this project. J. L. Fick prepared most of the figures appearing in the text, and H. Stapp and R. J. Riddell gave many helpful suggestions in the development of the modified theory.

The assistance of E. J. Lynch, C. d'A. Hunt, W. Dong, E. I. Motte, A. W. Peterson, L. J. Hov, and Mr. and Mrs. R. B. Waite, Harriet Powers, Esther Fenske, H. N. Pratt and C. E. Bacon and support to J. E. Powers by Socony Mobil Oil Corporation during part of the work are gratefully acknowledged.

This work was conducted under the sponsorship of the Radiation Laboratory.

NOTATION

a, a', a'' = general constants

A = area of the working space in a thermogravitational column (BL_T)

B = column width when $B_e = B_s$

B^* = optimum value of the column width, obtained from Equation (33a)

B_e, B_s = column width in the enriching section, stripping section

b, b' = general constants

C_1, C_2 = fraction of component 1, 2 in a binary solution

C_e, C_s = fraction of component 1 in the product stream exiting from the enriching section, stripping section

C_F = fraction of component 1 in the feed stream

D = ordinary-diffusion coefficient

e = subscript used to identify variables in enriching section ($y > 0$)

F = subscript used to identify feed properties

g = acceleration due to gravity

H = parameter evaluated by Equation (11)

$H^{(0)}$ = H for a column with no net flow of material through the working space [Equation (7a)]

$h(\omega\gamma)$ = correction term Equation (12)

$h_1(\omega\gamma)$ = use of the first term in the series defined by Equation (12)

J_{x-TD} = flux of component 1 in the x direction due to thermal diffusion

J_{x-OD}, J_{y-OD} = flux of component 1 in the x, y direction due to ordinary diffusion

K = $K_c + K_d + K_P$

K_c = $K_c^{(0)} k(\omega\gamma)$

$K_c^{(0)}$ = K_c for a column with no net flow of material through the working space

K_d = parameter defined and evaluated by Equation (7d)

K_P = a term appended to the mathematical treatment to account for the effects of parasitic remixing

$k(\omega\gamma)$ = correction term Equation (14)

$k_5(\omega\gamma)$ = use of the first five terms in the series defined by Equation (14)

L_e, L_s = length of the enriching, stripping section

L_T = total column length

m_0 = $(\partial\Delta/\partial\sigma)_{\sigma=0}$

n = index number used in Equation 14

p_e = power costs per unit area (sq. cm.) per unit time (day) for an apparatus with transfer plates at unit distance (cm.)

q = equilibrium separation factor for a thermogravitational column, $C_e(1 - C_s)/C_s(1 - C_e)$

S = amount of fixed charges per unit area (sq. cm.) per unit time (day).

s = subscript used to identify variables in the stripping section ($y < 0$)

T = absolute temperature

$\bar{T}$ = arithmetic average of the hot- and cold-plate temperatures

t = time

$v(x)$ = general velocity distribution function

x = axis normal to the plates

y = axis parallel to the plates in the direction of normal convective flow

Greek Letters

α = thermal-diffusion constant

β_T = $-\partial\rho/\partial T$

γ = parameter defined by Equation (9) and evaluated by Equation (15)

Δ = difference of concentrations at the ends of a thermogravitational column at steady state

Δ_0 = difference of concentrations at the ends of a thermogravitational column at steady state with no net flow of material through the working space

ΔT = difference in temperature of the hot and cold plate

η = coefficient of viscosity

θ = angle of the plates of a thermogravitational column from the vertical

λ = index number used in Equations (12) and (14)

π = total cost of operating a thermal-diffusion plant per unit time (day)

ρ = density

σ = $(\sigma_e + \sigma_s)/2$

σ_e, σ_s = mass flow rate out the enriching, stripping section

σ_F = mass flow rate of the feed stream

$(\sigma)_l$ = mass flow rate beyond which Equation (8) does not represent the data

$\psi(y)$ = relation defined by Equation (9)

ω = one half of the distance between the plates of a thermogravitational column

$2^*\omega$ = optimum value of the plate spacing obtained from Equation (30)

LITERATURE CITED

1. Bijl, A., *Ned. Tijdschr. Natuurk.*, **7**, 147 (1940); B. N. Cacciapuoti, *Nuovo cimento*, **18**, 114 (1941); R. H. Davis and J. T. Kendall, *Proc. Intern. Congr. Pure and Appl. Chem. (London)*, **11**, 429 (1947); H. Fleischmann and H. Jensen, *Ergeb. exakt. Naturw.*, **20**, 121 (1942); K. E. Grew and T. L. Ibbs, "Thermal Diffusion in Gases," Cambridge University Press, Cambridge (1952); G. S. Hartley, *Trans. Faraday Soc.*, **27**, (1931); Kozo Hirota, *J. Chem. Soc. (Japan)*, **63**, 292 (1942); J. A. Hveding, *Tidsskr. Kjemi Bergvesen Met.*, **1**, 110 (1941); H. Hensen, *Angew. Chem.*, **54**, 405 (1941); R. E. Kirk and D. F. Othmer, "Encyclopedia of Chemical Technology," pp. 115–124, The Interscience Encyclopedia Company, New York (1950); A. N. Murin, *Uspekhi Khim.*, **10**, 671 (1941); T. H. Osgood, *J. Appl. Phys.*, **15**, 89 (1944); K. Schafer, *Naturwissenschaften*, **34**, 104, 137, 166 (1947); Eiichi Takeda, *Bull. Tokyo Inst. Technol.*, **13**, 137; A. J. E. Welch, *Sci. J. Roy. Coll. Sci.*, **11**, 19 (1941).
2. Chilton, C. H., *Chem. Eng.*, **56**, no. 6, 97 (June, 1949).
3. Clusius, K., and G. Dickel, *Naturwissenschaften*, **26**, 546 (1938).
4. Dufour, L., *Arch. Sci. phys. et nat.* **45**, 9 (1872); *Pogg. Ann.*, **148**, 490 (1873); *Ann. Physik* [5], **28**, 490 (1873).
5. DeGroot, S. R., thesis, Univ. Amsterdam (1945).
6. Franke, G., *Ann. Physik*, **14**, 675 (1932).
7. Furry, W. H., R. C. Jones, and L. Onsager, *Phys. Rev.*, **55**, 1083 (1939).
8. "International Critical Tables," McGraw-Hill Book Company, Inc., New York (1928).
9. Jones, A. L., *Petroleum Processing*, **6**, 132 (February, 1951).
10. Jones, R. C., and W. H. Furry, *Rev. Modern Phys.*, **18**, 151 (1946).
11. Krasney-Ergen, William, *Phys. Rev.*, **58**, 1078 (1940).
12. Lemonde, H., *Compt. rend.* **202**, 468, 731, 1069 (1936).
13. Nier, A. O., *Phys. Rev.* **57**, 30 (1940).
14. Powers, J. E., Univ. Calif. Radiation Lab. Rept., UCRL-2618 (August, 1954).
15. Rakshit, J. N., *Z. Elektrochem.*, **32**, 276 (1926).
16. Smith, I. E., and J. A. Starrow, *J. Appl. Chem. (London)*, **2**, 225 (1952).
17. Trevoy, D. J., and H. G. Drickamer, *J. Chem. Phys.*, **17**, 582 (1949).
18. *Ibid.*, 1117 (1949).

Presented at A.I.Ch.E. Detroit meeting